JOURNAL OF CATALYSIS **169,** 212–227 (1997)
ARTICLE NO. CA971691

Carbon Deposition on Iron–Nickel during Interaction with Carbon Monoxide–Hydrogen Mixtures

C. Park,* N. M. Rodriguez,* and R. T. K. Baker*,†

Catalytic Materials Center, Materials Research Laboratory, The Pennsylvania State University, University Park, Pennsylvania 16802

Received June 13, 1996; revised March 12, 1997; accepted March 14, 1997

We have found that the composition of Fe–Ni catalysts can have a profound effect on the activity for the decomposition of CO/H_2 mixtures at 600°C. As the fraction of nickel in the bimetallic is increased above 70% there is a significant decline in the percentage conversion of CO. The amount of solid carbon deposited on a given bimetallic catalyst was shown to increase as the hydrogen content in the reactant mixture was raised to between 20 to 30% and then exhibited a steady decline with further addition of hydrogen. It was also evident that the structure and crystalline perfection of the carbon filaments that are produced during the reaction were very sensitive to the ratio of the two components in the catalyst. Temperature programmed oxidation and TEM studies of carbon filaments grown from various Fe–Ni bimetallic particles demonstrates that as the nickel content of the catalyst is increased there is a concomitant decrease in the crystalline perfection of the deposited carbon structures. These features are rationalized according to the notion that the addition of nickel to iron results in a reconstruction of the particle surfaces that leads to a diminution in the likelihood of iron atoms being nearest neighbors and the generation of atomic arrangements at carbon precipitating faces that do not favor the formation of graphite platelets in the deposited filamentous structures. A reversible deactivation process was shown to exist for all these Fe–Ni catalysts. At temperatures of about 725°C, the growth of carbon filaments suddenly ceased; however, restoration of catalytic activity could be readily achieved by lowering of the temperature to a previously active regime. Possible reasons for this unusual behavior are presented. © 1997 Academic Press

INTRODUCTION

The formation of carbonaceous deposits from the catalytic decomposition of carbon-containing gases, usually in the presence of hydrogen, is a highly complex phenomenon. For many years research concentrated on minimizing or stopping this detrimental deposition as it led to catalyst deactivation (1, 2) and, therefore, meant the renewal of the catalyst or costly regeneration procedures. Over the last decade, in direct contrast to the deleterious effects, the unique physical and chemical properties of filamentous carbon have led to an increased interest in the growth and potential applications of this type of material (3).

Filamentous carbon is produced when a hydrocarbon, or carbon monoxide molecule, is adsorbed on specific faces of the metal catalyst and decomposes to form carbon species, which subsequently diffuse through the particle and eventually precipitate at certain other faces to generate a fibrous structure. This process leaves the active metal faces free of solid carbon deposits and therefore available to undergo further reactions. The major advantage of this type of carbon growth is that the catalyst is able to accumulate large amounts of carbon and yet still maintain a constant activity over a prolonged period of time (4–8). If the sequence of events outlined above does not take place, then the deposited carbon tends to encapsulate the active metal sites and this behavior leads to rapid deactivation of the catalyst.

Carbon filaments have been previously grown from the catalytic decomposition of various carbon containing gases, e.g., ethylene, methane, or carbon monoxide, over the transition metals, iron, cobalt, and nickel (4, 5). More recently, much attention has been focused on the production of carbon filaments from bimetallic catalysts (6–10). Extensive studies by Baker and coworkers (11–14) using a variety of bimetallic catalysts and carbon containing gases have established that it is possible to tailor the structural characteristics of this material. These workers have demonstrated that the composition and nature of the bimetallic catalyst in conjuction with the carbon-containing gas and reaction conditions has a dramatic impact on the production and the crystalline perfection of the carbon filaments. The beneficial catalytic effects of introducing either certain metallic or nonmetallic adatoms to the host metal have been rationalized by a combination of geometrical and electronic effects.

It has been reported that iron has the ability to generate carbon filaments in large quantities from the decomposition of carbon monoxide in the presence of hydrogen at 600°C, which are comprised of graphite platelets oriented perpendicular to the fiber axis (13, 14). On the other hand,

---

*Authors' present address: Department of Chemistry, Hurtig Hall, Northeastern University, Boston, MA 02115.

†Author to whom all correspondence should be addressed.

0021-9517/97 $25.00

very few carbon filaments are produced on nickel under the same reaction conditions, and in this case the material tends to adopt a tubular structure where the graphite planes are aligned parallel to the axis of the fiber (5, 6, 15–20). Based on these diverse behavioral patterns it would constitute an intriguing challenge to predict the behavior of iron–nickel particles, with regard to the catalytic decomposition of carbon monoxide and the characteristics of the concomitant carbon deposition reaction. Extensive use is made of these metals as catalysts in a number of industrial processes, with the best known being the Fischer–Tropsch synthesis and methanation, and steam reforming processes. Carbon deposition during the Fischer–Tropsch reaction is known to exert a strong influence on both the selectivity and activity of these catalysts (21, 22) and, therefore, by combining the qualities of iron and nickel it is possible that the carbon deposition and, as a consequence, the selectivity of the catalyst can be controlled to a greater extent.

Another very important related use of iron and nickel is in the manufacture of steel alloys, materials that are used extensively throughout research and industry. One example of such an application is in steam cracking of paraffin feed stocks to produce olefins, a reaction that is performed by passage of the gases through steel reactor tubes at about 850°C. While this process itself does not involve the use of a catalyst, the iron and nickel constituents present in the alloy readily undergo reaction with the unsaturated gaseous products to form solid carbon (23). The accumulation of carbonaceous deposits on the tube walls reduces heat transfer properties and normally limits the reaction time, before the cracking tube must be taken off-stream for decoking (24, 25).

The deposition of carbon generated during the interaction of carbon monoxide with iron and nickel catalysts has been examined both in the presence and absence of added hydrogen (26–28). The conclusion reached from these studies was that the difference in behavioral characteristics exhibited by iron and nickel catalysts during interaction with carbon monoxide reactions was probably related to variations in the manner by which the gaseous reactant adsorbed on the respective metal surfaces. The coadsorption of carbon monoxide and hydrogen has also been comprehensively studied on selected transition metals (29–33). It was generally agreed that adsorption of the two gases on the surface of transition metals resulted in the formation of an unidentified surface complex species in the coadsorbed layer.

In the current investigation, we have examined the activity of a series of iron–nickel catalysts when reacted with carbon monoxide in the presence of hydrogen at temperatures over the range 500 to 750°C. Attention has been focused on both the gas phase and solid carbon product distributions, in conjunction with the subtle changes in the structural characteristics of the carbon filaments as a function of the catalyst composition, reaction temperature and CO/H_2 ratio. It was anticipated that the utilization of a bimetallic might result in geometrical and/or electronic perturbations in the system and such effects would be manifested by significant changes in the catalytic performance, possibly leading to the appearance of new properties that were not exhibited by either of the individual metals.

EXPERIMENTAL

Materials

The iron–nickel catalyst powders used in these studies were prepared by the coprecipitation of the metal carbonates from the respective metal nitrate solutions using ammonium bicarbonate as described in detail by Best and Russell (34). The precipitate was dried overnight in an oven at 100°C before being calcined in air at 400°C for 4 h to convert the carbonates into mixed metal oxides. The calcined catalyst was then reduced in a 10% H_2/He mixture for 20 h at 400°C. The reduced catalyst was subsequently cooled to ambient temperature in a helium atmosphere before being passivated in a 2% O_2/He mixture for 1 h at room temperature. The passivated catalyst was then removed from the reactor and stored for later use. Both the pure iron and nickel powders were prepared using a similar procedure.

The gases used in this work, hydrogen (99.999%), carbon monoxide (99.9%), and helium (99.99%), were obtained from MG Industries and used without any further purification. Reagent grade iron nitrate ($Fe(NO_3)_3 \cdot 9H_2O$) and reagent grade nickel nitrate ($Ni(NO_3)_2 \cdot 6H_2O$) were obtained from Fisher scientific for the catalyst preparation.

Apparatus and Procedures

The apparatus used throughout this study has been described previously (11). Briefly, the system consists of a quartz flow reactor heated by a conventional Lindberg horizontal tube furnace. The gas flow to the reactor is precisely monitored and regulated by use of MKS mass flow controllers allowing a constant composition of feed to be delivered. Powdered catalyst samples (50 mg) were placed in a ceramic boat at the center of the reactor tube in the furnace. After reduction in a 10% H_2/He mixture for 2.0 h at the desired reaction temperature the system was flushed with helium for 1.0 h. The reactant gas, CO, or a predetermined CO/H_2 mixture, was then allowed to flow over the catalyst for periods of up to 3.5 h. The reaction was followed as a function of time by sampling both the inlet and outlet gas streams at regular intervals and analyzing the reactants and products by gas chromatography using a 30-m megabore (GS-Q) capillary column in a Varian 3400 GC. The total amount of carbon deposited during the time on stream was determined gravimetrically after the system has been cooled to ambient temperature.

The nature and characteristics of the solid carbon were established using a combination of techniques, including high resolution transmission electron microscopy, temperature programmed oxidation in CO_2, X-ray diffraction, and surface area measurements. The TEM studies were performed in a JOEL 100 CX electron microscope fitted with a pole piece capable of giving a lattice resolution of 0.24 nm. Suitable transmission specimens were prepared by ultrasonic dispersion of sections of the carbon deposit in isobutanol and then a drop of the resultant suspension was applied to a holey carbon support grid. Examination of such deposits showed that in all cases the major component was filamentous carbon. In a further set of experiments the size of distributions of catalyst particles associated with the carbon filaments was determined from measurements of over 300 particles from each sample.

Thermogravimetric analysis of carbon filaments was carried out using a Cahn 2000 microbalance in the presence of CO_2 at a constant heating rate. Prior to oxidation all metallic inclusions were removed from the filaments by repeated washing in 1*M* HCl over a period of 7 days. This is a necessary operation since the presence of metals has been shown by Baker and co-workers (35) to have a profound effect on the rate of gasification of the carbon filaments and graphite. Nickel, in particular, was shown to be a very active catalyst for the gasification of both carbon filaments and graphite in CO_2. Under these conditions high purity amorphous carbon, starts to undergo gasification at 675°C, whereas the onset for removal of graphite carbon does not place until the temperature is raised to 850°C. By comparison of the oxidation profiles of a given batch of carbon filaments with those of amorphous carbon and graphite it is a relatively simple task to determine the fraction of highly crystalline carbon in the deposited material.

Powder XRD patterns of the starting Fe–Ni catalyst powders and the carbon filaments were obtained with a Scintag diffractometer using nickel filtered Cu Kα radiation. Diffraction patterns were recorded over a range of 2θ angles from 10 to 90° and compared with the known X-ray powder files to establish the phase identities. Finally, BET surface areas of the carbon deposits, calculated from the nitrogen adsorption isotherms at −196°C, and static carbon monoxide chemisorption measurements of Fe–Ni powders were carried out using a Coulter Omnisorb 100CX unit.

RESULTS

1. Flow Reactor Studies

1.1. Effect of Catalyst Composition on the Gas and Solid Phase Product Distributions

The effect of changing the ratio of the components in the bimetallic catalyst on the gas phase product distribution from the decomposition of a CO/H_2 (4 : 1) mixture at 600°C is presented in Fig. 1. The conditions for all the catalyst samples were identical and reactions were allowed to proceed for a period of 3.5 h. As expected the three main gaseous products of this reaction were identified as being CO_2, H_2O, and CH_4. Catalysts powders with a composition of up to and including 70% Ni displayed a similar product distribution. As the fraction of nickel in the catalyst is progressively raised to higher levels then a dramatic decrease in the percent decomposition of CO is observed. A somewhat more accurate assessment of the relative activities of these catalyst systems can obtained from a comparison of the respective turnover frequencies (TOF) that are presented in Table 1.

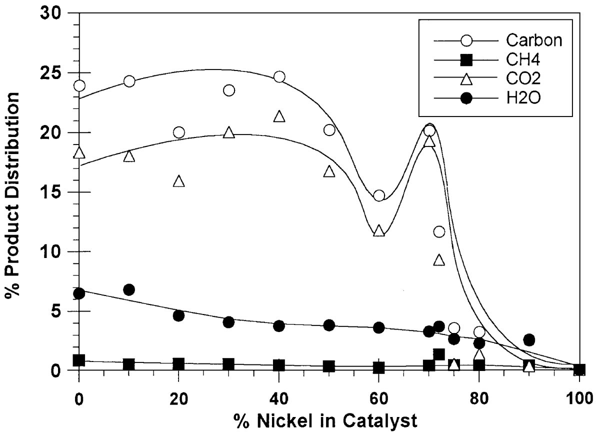

FIG. 1. The percentage product from the decomposition of CO/H_2 (4 : 1) over various Fe–Ni powders at 600°C.

These values have been calculated from the following expression:

$$\mathrm{TOF}_{\text{minimum}}\ (\mathrm{s}^{-1}) = \frac{\text{Reaction rate } (\mu\text{mol/g}_{\text{cat}} \cdot \text{s}) \cdot \text{Molecular Wt. of Metal} \cdot 10^{-6}}{\text{Wt. fraction of metal in catalyst} \cdot \text{d}_{\text{s}}},$$

where

$$\text{Reaction rate} = \frac{\mu\text{mol/s of CO converted}}{\text{Wt. of catalyst (g)}}$$

TABLE 1

Rates of Reaction and Turnover Frequencies for the Interaction of Various Fe–Ni Catalysts with a CO/H_2 (4 : 1) Mixture at 600°C

Fe–Ni ratio	Reaction rate (μmol/g · s)	Dispersion (μmol/g)	TOF (1/s)
9 : 1	184.8	548.1	0.337
6 : 4	186.7	370.9	0.503
4 : 6	112.3	560.4	0.200
3 : 7	160.0	421.6	0.379
1 : 9	21.5	1600.0	0.013

and

$$d_s = \frac{\text{Metal at Particle Surface}}{\text{Total Metal}} = \frac{1.217\ (\text{nm})}{\text{Average Particle Width (nm)}}.$$

In the calculation of d_s we have used a value of 0.352 nm for the lattice parameter of the metal and the average metal particle widths were determined from the TEM measurements. We have assumed a spherical morphology for the "average" shape of crystallites associated with the carbon filaments. This latter approach may be subject to error, since a TEM examination is only 2D in nature and we do not know the fraction of the metal surface that is actually involved in the gas phase decomposition reaction. Unfortunately, attempts at determining metal surface areas by standard chemisorption methods were thwarted by the presence of the carbon deposit.

The amount of solid carbon produced during the reaction was determined gravimetrically and this value was used to compare the activity of the various catalyst compositions. It was found that the weight of carbon obtained from catalyst compositions of up to and including 70% Ni were comparable, being in the range of 1.0 to 1.6 g. When the concentration of nickel in the bimetallic was increased above 70% then, in a analogous fashion to the gas phase product distributions, there was a precipitous drop in the amount of solid carbon formed in the reaction.

1.2. *Influence of Hydrogen on Carbon Deposition*

The effect of adding increasing amounts of hydrogen to the CO feed on the formation of filamentous carbon over selected Fe–Ni catalysts at 600°C is shown in Fig. 2. It is apparent that the amount of solid carbon increased as the hydrogen content in the reactant was raised to between 20 to 30% and thereafter exhibited a steady decline with further addition of hydrogen. Bimetallic powders containing 75% or more nickel exhibited low CO conversions, which in turn accounts for the very limited amounts of carbon filaments produced when compared with those obtained from powders with a lower Ni content. For all Fe–Ni catalysts investigated, it was found that as the concentration of hydrogen in the feed was gradually raised there was a corresponding increase in the conversion of CO to both methane and water. In contrast, however, the yield of carbon dioxide, like that of solid carbon, decreased as the hydrogen content in the reactant gas was increased above 30%. Examples of these trends are presented in Table 2 for the decomposition of various CO/H_2 mixtures over Fe–Ni (6 : 4) and Fe–Ni (4 : 6) powders at 600°C.

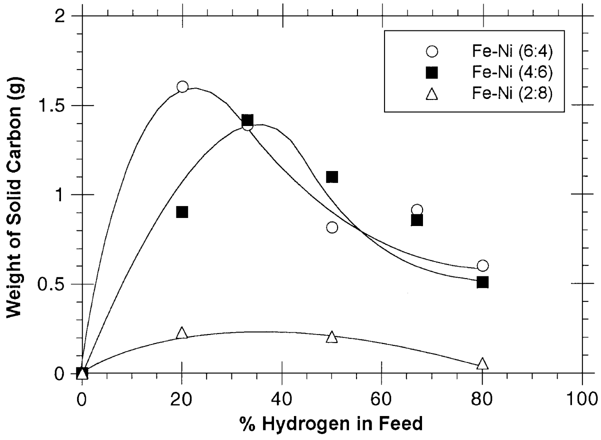

FIG. 2. Effect of hydrogen on the weight of solid carbon from the Fe–Ni catalyzed decomposition of CO at 600°C (reaction time 1.5 h).

TABLE 2

Percentage Product Distribution for Selected Fe–Ni Catalysts as a Function of the Percentage of H_2 in the CO Reactant at 600°C

H_2 in CO (%)	Product (%)	Fe–Ni (6 : 4)	Fe–Ni (4 : 6)
20	CH_4	0.44	0.22
	CO_2	21.36	11.27
	H_2O	3.72	3.58
	Solid carbon	22.41	14.34
30	CH_4	1.36	1.42
	CO_2	16.82	18.07
	H_2O	14.99	16.32
	Solid carbon	22.31	23.08
50	CH_4	4.89	3.00
	CO_2	12.24	14.45
	H_2O	17.86	20.56
	Solid carbon	15.13	18.75
60	CH_4	8.69	6.53
	CO_2	9.90	8.61
	H_2O	40.99	40.33
	Solid carbon	14.52	16.37
80	CH_4	17.10	17.90
	CO_2	6.37	6.20
	H_2O	40.99	41.50
	Solid carbon	14.52	15.87

In an attempt to ascertain the origin of the relatively large amount of methane produced in systems containing high concentrations of hydrogen in the reactant, an experiment was performed in which an Fe–Ni (2 : 8) powder was treated in CO/H_2 at 600°C for approximately 100 min and the gaseous products analyzed at regular intervals. The addition of CO to the bimetallic was then stopped at this particular time so that H_2 was the only reactant present. The results of this operation are presented in Fig. 3, where it is evident that the formation of methane exhibits a rapid increase as CO is removed from the system. This sequence of events suggests that a significant amount of the methane

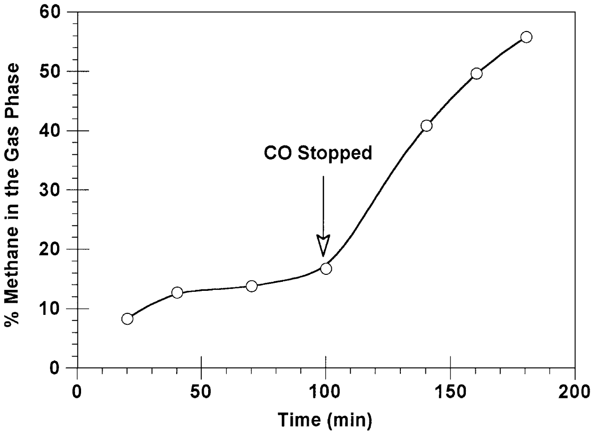

FIG. 3. The percentage of methane formed from the interaction of an Fe–Ni (2 : 8) catalyst with a CO/H_2 (1 : 4) mixture at 600°C.

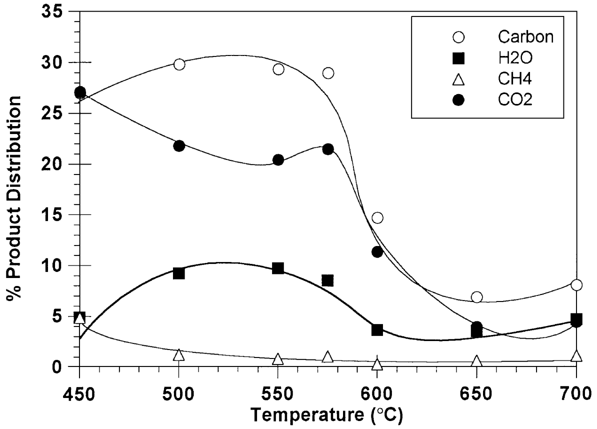

FIG. 5. Variation in the percentage product distribution as a function of reaction temperature for the decomposition of CO/H_2 (4 : 1) over an Fe–Ni (4 : 6) catalyst.

that is formed under conditions where the reactant mixture contains a large fraction of H_2 is generated from the hydrogasification of solid carbon.

1.3. Effect of Reaction Temperature on the Product Distributions

The reaction temperature was found to have a profound effect on both the product distribution and on the nature of the carbon filaments produced on Fe–Ni catalysts from the decomposition of a CO/H_2 (4 : 1) mixture. Examples of this dependence are shown for two selected catalyst compositions, Fe–Ni (6 : 4) and Fe–Ni (4 : 6), in Figs. 4 and 5, respectively. It is evident in both systems that at temperature below 500°C, there is a substantial conversion of CO to both CO_2 and solid carbon and also a relatively large yield of H_2O and CH_4. As the temperature is progressively raised to 575°C for the Fe–Ni (4 : 6) and 600°C for the Fe–Ni (6 : 4) samples, there is a significant decrease in the conversion to CH_4 while that to CO_2 and solid carbon tends to remain relatively constant. On continued heating up to 700°C the overall conversion of CO exhibits a steep decline and eventually settles down to a steady level. At this upper limit the catalytic decomposition of CO is very low and although solid carbon is still the major product, the actual amount that is deposited on the surfaces of the bimetallics has dropped substantially.

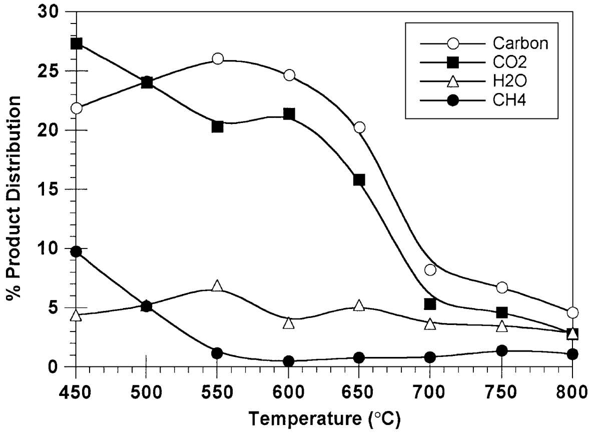

FIG. 4. Variation in the percentage product distribution as a function of reaction temperature for the decomposition of CO/H_2 (4 : 1) over an Fe–Ni (6 : 4) catalyst.

1.4. Deactivation Phenomenon Associated with High Temperature Treatment of Fe–Ni Catalysts

As noted in the previous section when the reaction temperature was increased above 650°C a dramatic drop was observed in both the formation of gaseous products and that of filamentous carbon. This behavior appeared to be most pronounced for the bimetallic powders containing relatively large amounts of nickel. In an attempt to establish a fundamental understanding of the factors surrounding this catalyst deactivation phenomenon a series of experiments was designed to ascertain the origin of this behavior. Initially the decomposition of CO reaction was conducted at 725°C, conditions where the catalyst would be expected to exhibit very limited activity. After a period of 60 min on stream, the temperature was gradually lowered to 600°C, a regime where in the previous experiments the performance of the bimetallic catalysts had been quite exceptional. The results of this sequence of steps are shown in Fig. 6 for two selected catalyst systems. Inspection of these data indicates that while both catalysts were initially in a deactivated state at 725°C, as the temperature was lowered to 600°C the conversion of CO very quickly increased and there was a corresponding enhancement in the formation of carbon filaments. In a further series of experiments the temperature was cycled between these two limits several times and on each occasion deactivation and restoration of the catalytic

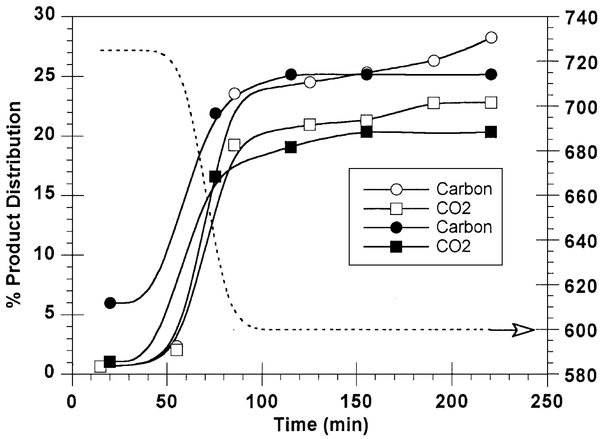

FIG. 6. Re-activation behavior of selected Fe–Ni catalysts during the decomposition of CO/H_2 (4 : 1) as the temperature is lowered from 725 to 600°C. The "open" symbols refer to product formation from a Fe–Ni (3 : 7) catalyst powder and the "filled in" symbols are those of the corresponding data for a Fe–Ni (6 : 4) sample.

effect was achieved, demonstrating the reversible nature of this deactivation phenomenon.

2. Characterization of the Carbon Deposits

2.1. *Transmission Electron Microscopy Studies*

Transmission electron microscopy examinations of the solid carbon deposits grown during the decomposition of carbon monoxide at 600°C in the presence of hydrogen on a range of iron–nickel catalyst powders revealed that they consisted almost entirely of filamentous structures. Comparison of the characteristics of the various batches of carbon filaments showed several very interesting traits. The most striking feature is the dependence of the filamentous carbon structure on the composition of the initial catalyst powder. The structures formed from a pure iron powder are generated via a whisker-like mode where the catalyst particle is situated at the end of the filament. High resolution examination shows that these filaments possess a well defined and ordered "platelet" structure where the graphite layers are stacked on top of each other in a perpendicular direction with respect to the fiber axis in a similar manner to "a deck of cards," Figs. 7a, b. As the amount of nickel is gradually increased, however, very subtle changes are observed in the characteristics of the carbon filaments. When as little as 10% nickel is added to iron then the majority of the filaments still possess the well ordered crystalline form, but under these circumstances there is a tendency for growth to occur by a bidirectional process, where the catalyst particle is entrenched within the filament. Figures 8a, b show the appearance of a filament produced from the interaction of a Fe–Ni (9 : 1) catalyst with CO/H_2 at 600°C and indicates that the material acquires a "herring-bone" structure, where the graphite platelets are aligned at an angle to the fiber axis and the lattice spacing is 0.34 nm, a value also found for the bulk material from XRD analysis. As the amount of nickel in the starting catalyst is increased, there is a concomitant enhancement in the number of filaments produced by the bidirectional mode.

Both of these types of carbon filaments are not expected to exhibit the same high values of tensile strength as those where the alignment of the graphite platelets is parallel to the fiber axis, since in the present cases the layers are held together by van der Waals forces and possibly some groups at edges may contribute towards maintenance of the structural integrity, whereas in the latter case, covalent bonding coupled with delocalized π-bonding is responsible for creating one of the strongest materials known to man. It is worth mentioning in this context that preparation of thin cleaved sections of single crystal graphite requires a certain degree of force to separate the layer planes.

The most outstanding modification in the carbon filament characteristics was observed from a comparison of the materials grown on Fe–Ni (30 : 70) and Fe–Ni (25 : 75) powders under the same reaction conditions. It was evident that by merely adding an extra 5% Ni to the catalyst, the structural conformation of the filaments tended to change from one where the graphite platelets were oriented in a "herring-bone" arrangement to that where the platelets were aligned parallel to the fiber axis and the filaments took the form of tubules, examples of which are presented in Figs. 9 and 10. It was significant that this transformation in filament structure correlated with the dramatic decrease in conversion of CO in the gas phase analysis. As the nickel content was increased further then the tubular conformation became the exclusive filament growth form. It is evident from these studies that the abrupt decrease in catalytic activity associated with the increase in nickel content of the bimetallic also has a direct impact on the structural characteristics of the carbon filaments that are produced during the CO decomposition reaction.

The size distributions of particles associated with the carbon filaments produced from the interaction of various Fe–Ni powders with CO/H_2 (4 : 1) mixtures at 600°C was determined from measurements of over 300 particles in each sample and examples of two such plots are presented in Figs. 11 and 12. The distribution profiles of particles derived from all the Fe–Ni bimetallics, with the exception of the Fe–Ni (1 : 9) powder, were similar and for the sake of brevity only those of the latter sample and Fe–Ni (6 : 4) are given. From analysis of all the data there does not appear to be any systematic trend with respect to the initial catalyst composition. From these distributions it has been possible to derive values for the weighted average particle sizes; Fe–Ni (9 : 1) = 32.5 nm; Fe–Ni (6 : 4) = 47.3 nm; Fe–Ni (4 : 6) = 31.0 nm; Fe–Ni (3 : 7) = 41.0 nm; and Fe–Ni (1 : 9) = 10.7 nm. It should be emphasized that these values

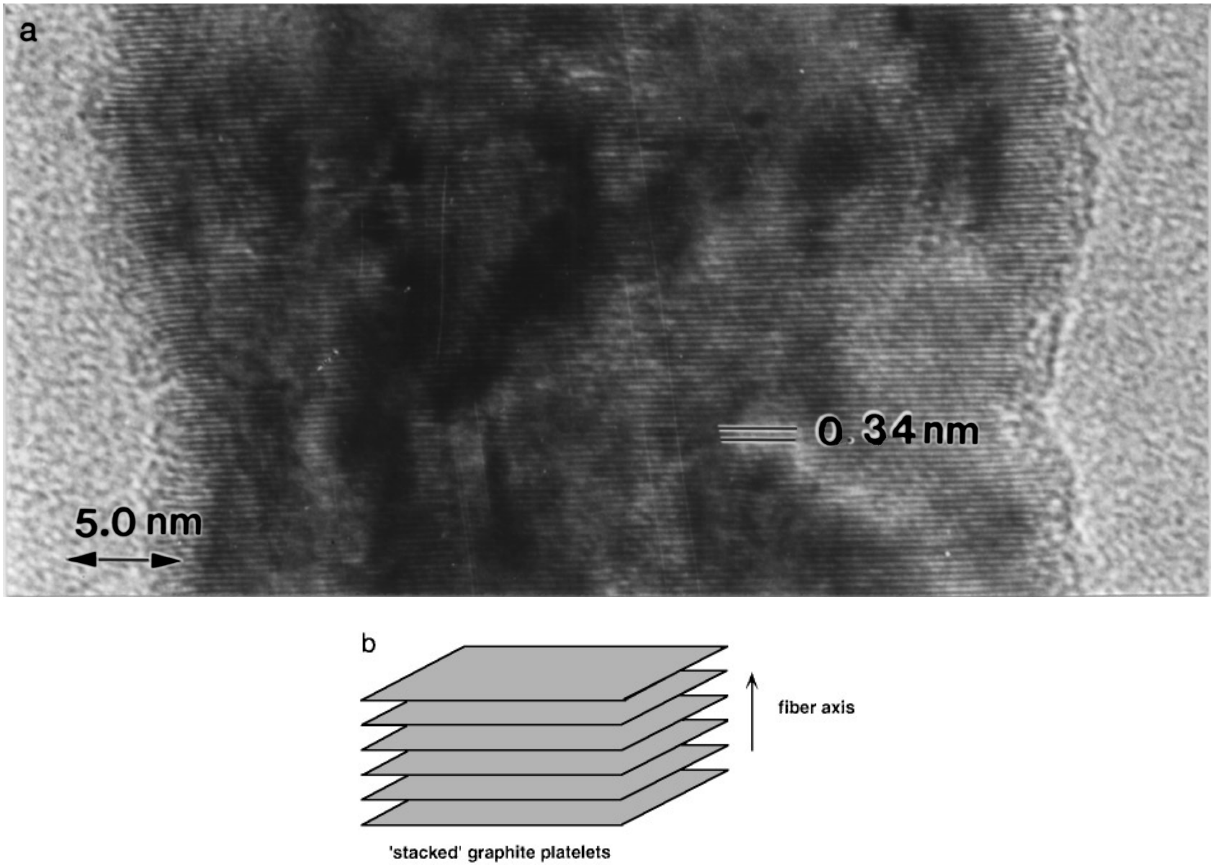

FIG. 7. a. High resolution electron micrograph of a section of a carbon filament produced from the Fe–CO/H_2 reaction at 600°C showing the appearance of graphite platelets stacked in an arrangement perpendicular to the fiber axis. b. Schematic representation of the graphite platelet stacking arrangement of the filament shown in a.

are determined after 3.5 h reaction and as such, do not represent the metal particle sizes at any particular instant in time. Indeed, as a given reaction proceeds the average particle size may exhibit a significant change. As a consequence, extreme caution must be exercised in drawing any conclusions from the values of the "turnover frequencies" presented in Table 1.

Examination of carbon filaments generated from the interaction of Fe–Ni (6 : 4) with mixtures containing various ratios of CO and H_2 at 600°C indicates that the metal catalyst particles tended to become more faceted as the hydrogen content was increased. While the conformational characteristics of the carbon filaments produced from this bimetallic did not appear to exhibit any changes, the degree of crystalline perfection improved significantly in the presence of excess hydrogen. On the other hand, the structural characteristics of carbon filaments produced from catalysts having a higher nickel content, Fe–Ni (4 : 6) and Fe–Ni (2 : 8), did undergo significant modifications when the feed composition was altered. As the fraction of hydrogen in the reactant gas was increased it was evident that a major portion of the material produced on these nickel-rich powders was in the form of tubules.

In a further series of TEM studies some very interesting features were revealed regarding the influence of reaction temperature on the structural and morphological characteristics of the carbon filaments generated from the decomposition of a CO/H_2 (4 : 1) mixture over an Fe–Ni (4 : 6) powder. At lower temperatures, 450 and 500°C, the carbon filaments consisted of a combination of relatively straight structures, where the graphite platelets were oriented either at an angle or perpendicular to the fiber axis, and a number of other filaments that took the form of spiral growths. At 600°C an extensive search of the many regions of the specimen showed that there was an abundance of the straight filaments, however, under these conditions no evidence for spiral conformations was detected. While straight filaments remained the exclusive growth form at 650°C, high resolution studies revealed the existence of a dramatic change in the orientation of the graphite platelets, which were now aligned in a direction parallel to the fiber axis, a characteristic associated with the tubular structure. Above this temperature the crystalline perfection of the deposit decreased quite sharply and the carbon filaments acquired a very ill-defined conformation. Indeed, many of the structures were shell-like in nature with the metal catalyst

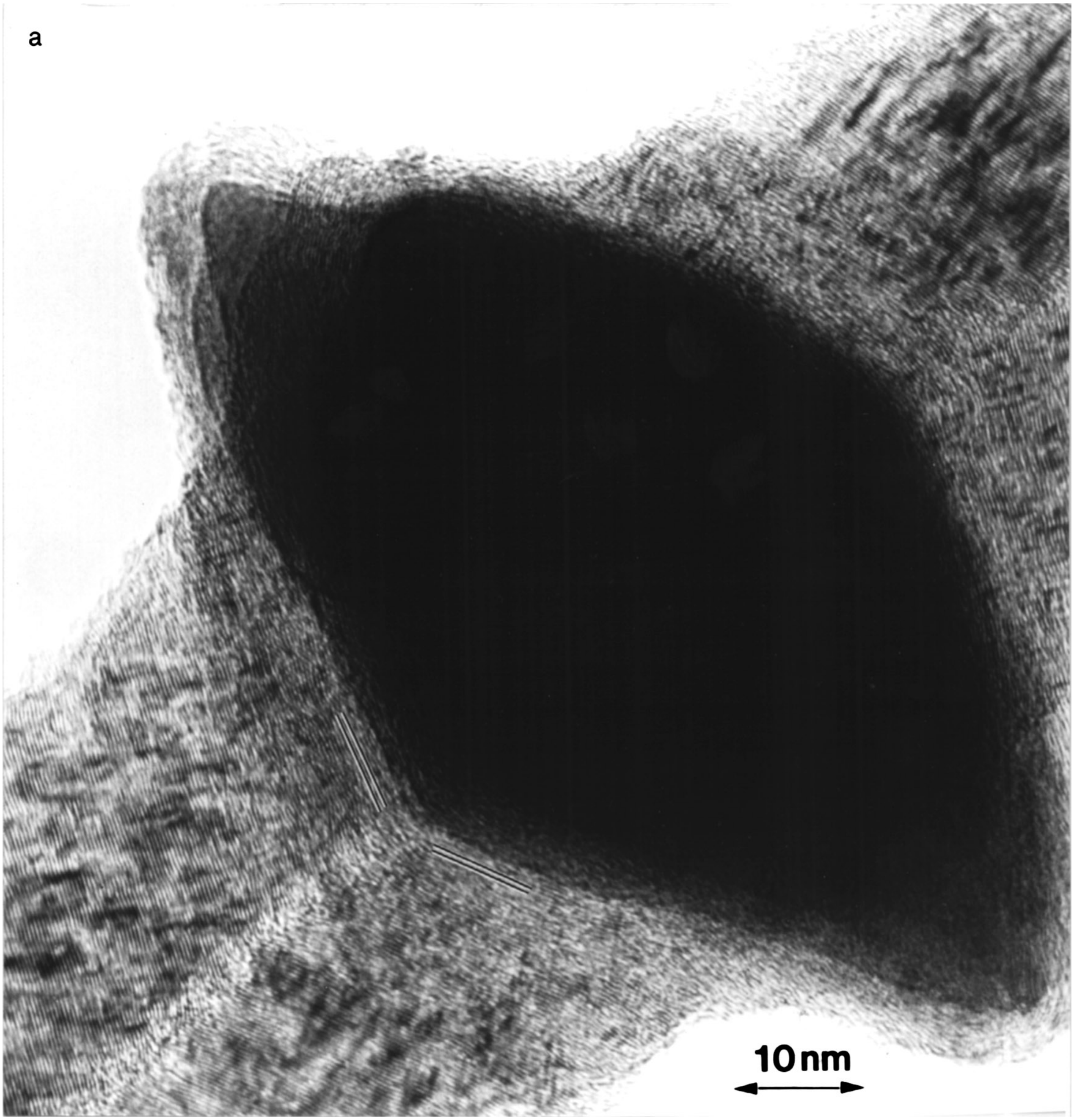

FIG. 8a. High resolution electron micrograph of a section of a carbon filament produced from the Fe–Ni (9 : 1)-CO/H_2 reaction at 600°C showing the appearance of graphite platelets stacked in a "herring-bone" arrangement.

particle appearing to be encased within the deposit. It is possible that the observed transition in both the orientation of graphite platelets and the overall degree of structural order of the carbon filaments is directly linked to modifications in the characteristics of the catalyst particles. It is not unreasonable to assume that not only the chemical state, but also the arrangement of atoms in the set of faces of the bimetallic particles where dissociation chemisorption of CO occurs and those at which carbon is precipitated in the form of graphite platelets to constitute the fibrous structures will exhibit major changes as the reaction temperature is progressively raised.

2.2. *Temperature Programmed Oxidation Studies*

The oxidation profiles of demineralized carbon filaments grown from the interaction of CO/H_2 (4 : 1) mixture with a selected number of Fe–Ni powders at 600°C for 3.5 h are

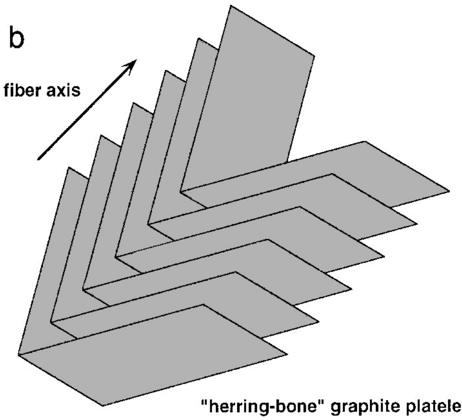

FIG. 8b. Schematic representation of the graphite platelet stacking arrangement of the filament shown in Fig. 8a.

compared with those for filaments produced from a pure iron powder when treated under the same conditions in Fig. 13. It is apparent that the oxidation profiles are found to be highly dependent upon the catalyst composition. Carbon filaments grown from iron exhibit the highest onset temperature for gasification and therefore the highest degree of crystalline order. In general, the structures produced from bimetallic powders with a high iron content were found to be more graphitic in nature than those grown from catalysts that were rich in nickel. These results are consistent with the observations made on individual carbon filaments from the transmission electron microscopy studies.

Temperature-programmed oxidation studies were also conducted on carbon filaments produced from a series of experiments where the composition of the bimetallic catalyst and reaction temperature were maintained constant, at Fe–Ni (6 : 4) and 600°C, respectively, but where there was an increase in the hydrogen content of the CO/H_2 reactant. The data obtained from these studies is presented in Fig. 14 and clearly indicate that as the fraction of hydrogen in the reactant is raised, the carbon filaments produced from the decomposition of CO become progressively more graphitic in nature.

In a final set of experiments, the influence of reaction temperature on the graphitic nature of the carbon filaments was investigated. For this purpose the composition of the catalyst and gaseous reactant were held constant at Fe–Ni (4 : 6)

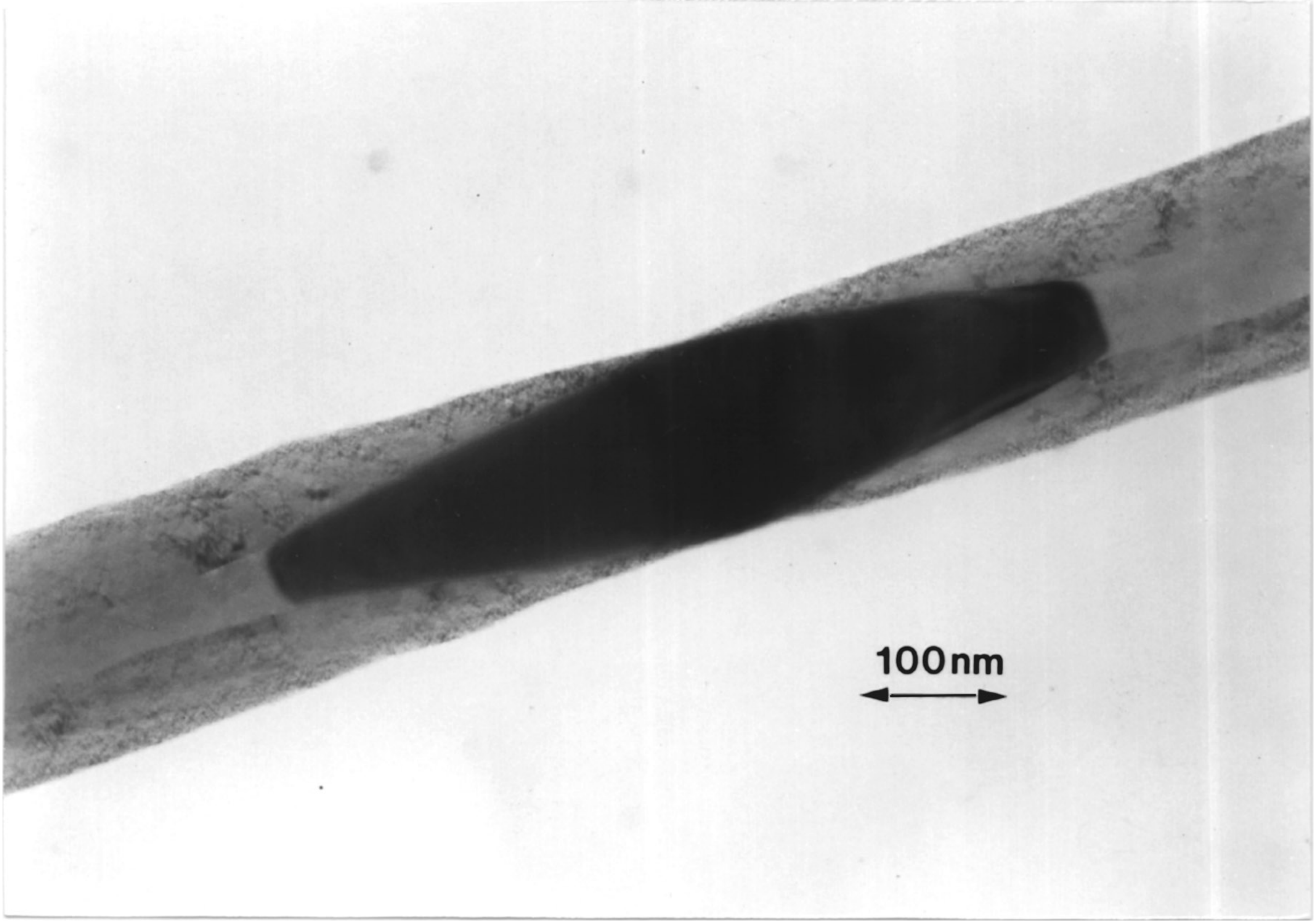

FIG. 9. Transmission electron micrograph showing the appearance of carbon filaments produced from the interaction of Fe–Ni (25 : 75) with CO/H_2 at 600°C.

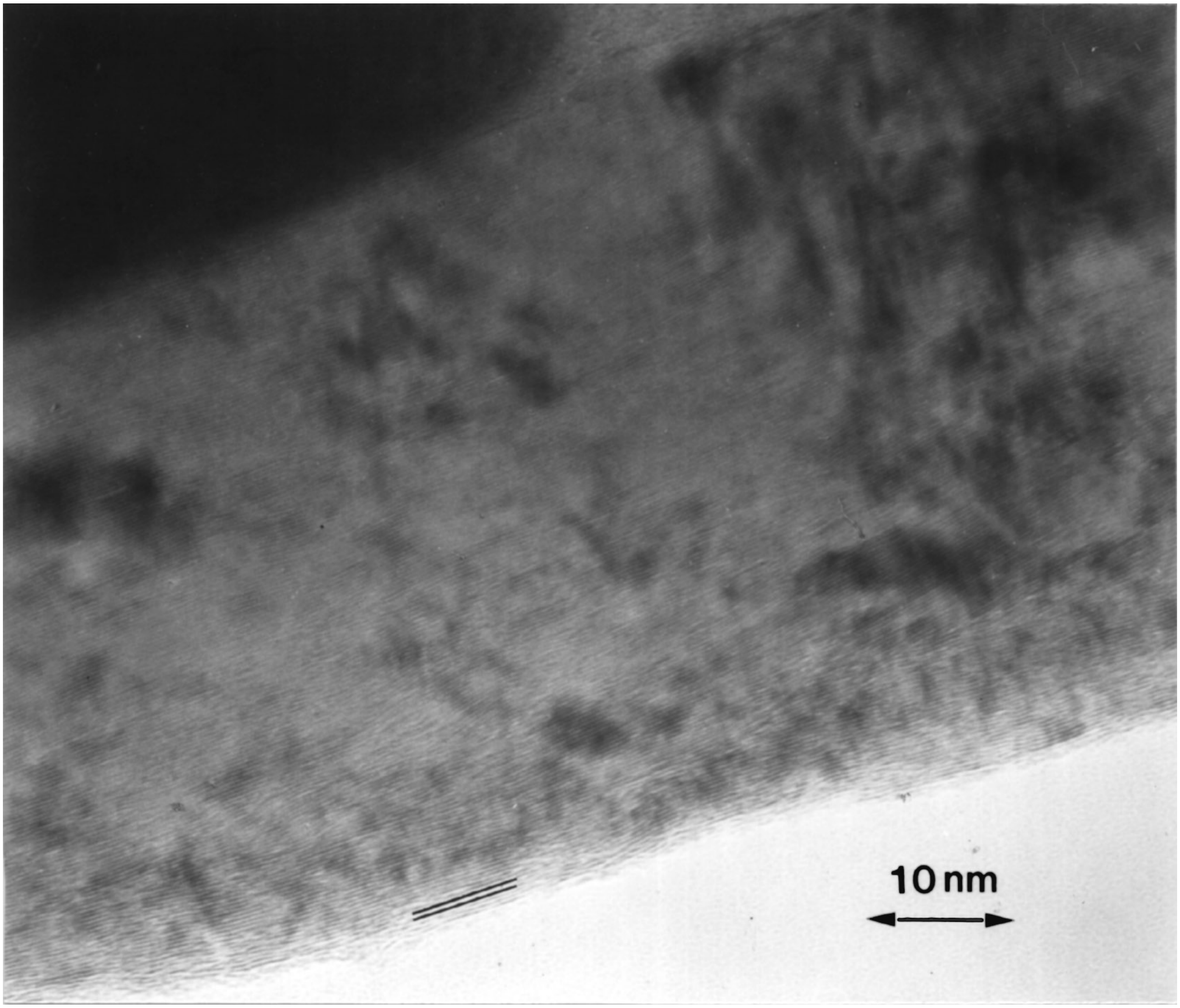

FIG. 10. High resolution electron micrograph of a section of a carbon filament produced from the Fe–Ni (25 : 75)-CO/H_2 reaction at 600°C showing the appearance of graphite platelets stacked in a direction parallel to the fiber axis.

and CO/H_2 (4 : 1), respectively, while the temperature was varied over the range 450 to 650°C. It is apparent from the data presented in Fig. 15 that the material acquires a more graphitic nature as the reaction temperature is increased, reaching an optimum level at 600°C. At even higher temperatures, the degree of crystalline order is substantially less than that of any of the filaments produced at or below 600°C.

2.3. Nitrogen BET Surface Area Measurements

The N_2 BET surface area measurements of the carbon filaments grown from the decomposition of a CO/H_2 (4 : 1) mixture over a range of Fe–Ni powders at 600°C are detailed in Table 3. It is evident that the structures grown from catalysts that are rich in Ni have much lower surface areas than those grown from powders where Fe is the major component. This trend is particularly marked when the composition of Ni in the catalyst was increased above 70%. This sudden decline in the surface area of the filaments coincides with the decrease in the activity of the catalyst and concurrent drop in the amount of the solid carbon deposit. It is clear, therefore, that not only the production, but also the structural characteristics of the carbon filaments are extremely sensitive to the catalyst composition.

In experiments where the concentration of hydrogen in the reactant was progressively raised it was found that N_2 BET surface area of the carbon filaments exhibited a uniform decrease. Examples of this trend are given for two bimetallic powders, Fe–Ni (6 : 4) and Fe–Ni (4 : 6) in Table 4. These data are consistent with the findings that the as the hydrogen content in the reactant was increased the filamentous structures appeared to become smoother, and in some cases the arrangement of graphite platelets changed from a condition where a large fraction of the edge sites would

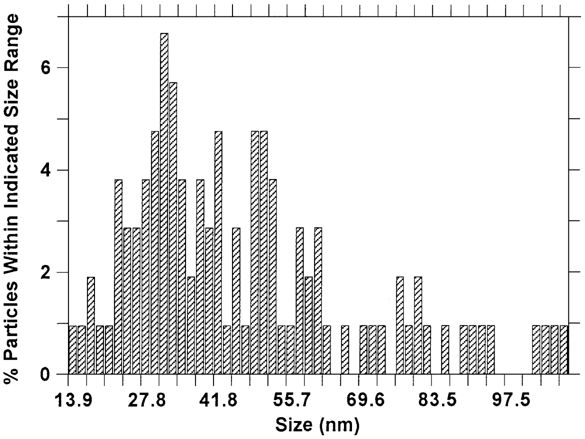

FIG. 11. Particle size distribution profile of catalyst particles associated with carbon filaments grown over a period of 3.5 h from the interaction of Fe–Ni (6 : 4) with a CO/H_2 (4 : 1) mixture at 600°C.

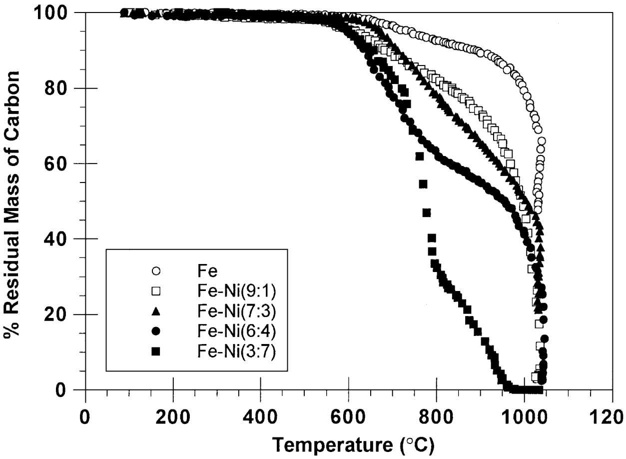

FIG. 13. Comparison of the gasification characteristics in CO_2 of carbon filaments produced from the interaction of various Fe–Ni powders with CO/H_2 (4 : 1) at 600°C.

be available for gas adsorption to one in which only the relatively inert basal plane regions were exposed.

Measurements of the N_2 BET surface areas of carbon filaments grown from the decomposition of a CO/H_2 (4 : 1) mixture over two selected bimetallic powders as a function of reaction temperature are presented in Table 5. In both cases it is apparent that the carbon structures grown at 500°C have a relatively high surface area of approximately 180 to 190 $m^2\ g^{-1}$. As the reaction temperature was increased to 600°C the surface area of the solid carbon structures decreased by about 50% and at higher levels there was a precipitous drop to levels of between 30 to 40 $m^2\ g^{-1}$. These values are not totally unexpected in view of the tendency for compact shell-like deposits to be produced at temperatures in excess of 650°C.

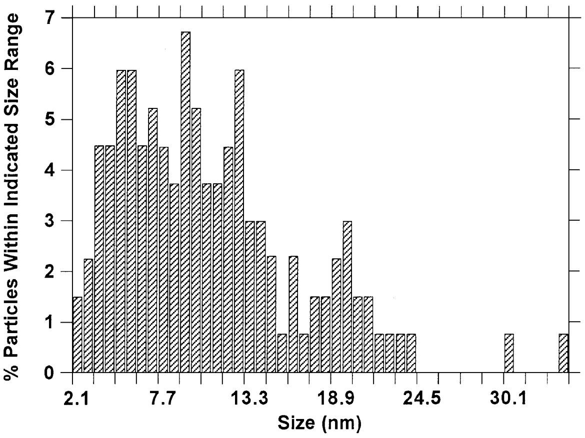

FIG. 12. Particle size distribution profile of catalyst particles associated with carbon filaments grown over a period of 3.5 h from the interaction of Fe–Ni (1 : 9) with a CO/H_2 (4 : 1) mixture at 600°C.

3. Characterization Studies of the Bimetallic Powders

3.1. *CO Chemisorption on Fe–Ni Powders*

Preliminary CO chemisorption studies of the Fe–Ni catalyst powders shows that there is a major difference in the behavior of the reduced powders having compositions of Fe–Ni (2 : 8) and (3 : 7). For the reduced catalyst powders, at ambient temperature, the interaction of carbon monoxide with both surfaces is very similar. Similar amounts of carbon monoxide were molecularly adsorbed and desorbed by both samples and there was no evidence under these conditions for dissociation of the adsorbed gas molecules. In contrast, when the reduced catalysts were exposed to carbon monoxide at 200°C, very different results were found. Once again very little or no dissociation of the carbon monoxide

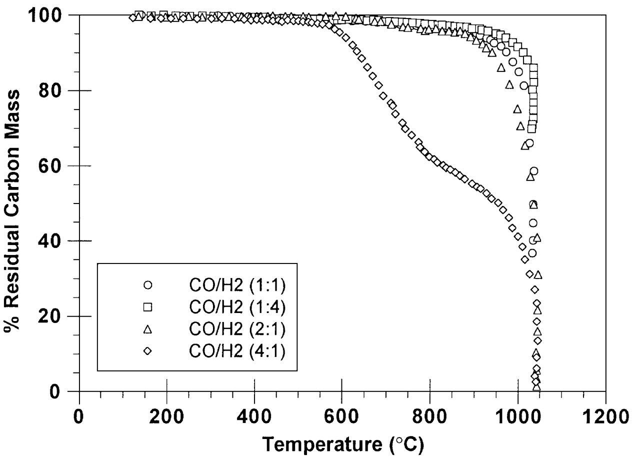

FIG. 14. Comparison of the gasification characteristics in CO_2 of carbon filaments produced from the interaction of Fe–Ni (6 : 4) with CO containing various amounts of added H_2 at 600°C.

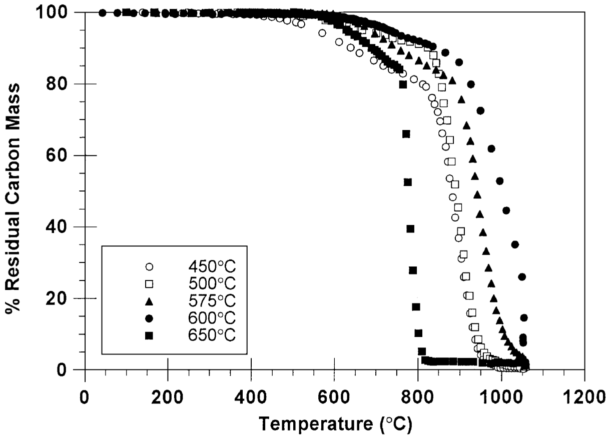

FIG. 15. Comparison of the gasification characteristics in CO_2 of carbon filaments produced from the interaction of Fe–Ni (4 : 6) with CO/H_2 (4 : 1) at temperatures over the range 450 to 650°C.

was found for the Fe–Ni (2 : 8) powder, adsorption once again taking place by a molecular mode. On the other hand, with the Fe–Ni (3 : 7) sample there were indications that some initial dissociation of the carbon monoxide occurred prior to molecular adsorption of the gas.

3.2. X-Ray Diffraction Studies of the Bimetallic Powders

XRD analysis of the passivated Fe–Ni bimetallic powders showed the existence of peaks that corresponded only to those of metallic iron and nickel. No peaks were found that could be assigned to the corresponding metal oxides in these powders at room temperature. This finding confirms the effectiveness of the passivation process that was conducted in 2% O_2/He after reduction. A further feature to emerge from this analysis was that at ambient temperature there was no substantial evidence for alloy formation, however, under reaction conditions the possibility of an interaction and even alloying between two metals cannot be ignored.

TABLE 3

Variation of the N_2 BET Surface Area of Carbon Filaments Produced from the Decomposition of CO/H_2 (4 : 1) over Different Fe–Ni Catalysts at 600°C

Catalyst composition	Surface area (m^2/g)
Fe	122.9
Fe : Ni (9 : 1)	90.4
Fe : Ni (8 : 2)	117.6
Fe : Ni (6 : 4)	94.7
Fe : Ni (4 : 6)	109.9
Fe : Ni (3 : 7)	83.2
Fe : Ni (2 : 8)	52.2
Fe : Ni (1 : 9)	14.9

TABLE 4

Variation of the N_2 BET Surface Area of Carbon Filaments Produced from the Interaction of Two Selected Fe–Ni Catalysts with Different CO/H_2 Mixtures at 600°C

CO/H_2 ratio	Fe : Ni (6 : 4) surface area (m^2/g)	Fe : Ni (4 : 6) surface area (m^2/g)
4 : 1	94.7	109.9
2 : 1	—	83.5
1 : 1	111.3	75.0
1 : 2	91.4	66.8
1 : 4	83.5	—

DISCUSSION

The results detailed in the previous section clearly indicate that the activity of the Fe–Ni catalysts and the structure and degree of crystalline order of the carbon filaments produced from the interaction of the bimetallics with CO/H_2 mixtures is highly dependent upon a number of factors, including the catalyst composition, the nature of the reactant gas, and the reaction temperature.

Effect of catalyst composition on carbon deposition. As illustrated in Fig. 1, there is a dramatic change in the activity for the decomposition of CO with these Fe–Ni catalysts in the composition range Fe–Ni (30 : 70) and (25 : 75). The addition of a mere 5% more nickel to a Fe–Ni (30 : 70) catalyst resulted in a dramatic decrease in the activity and a percentage conversion to all major products. These findings are consistent with data reported by Vreeburg and co-workers (8, 9) who studied the interaction of CO with $Ni_{(111)}$–Fe alloys and found a comparable change in the activity of the system in the when the fraction of iron in the catalyst was less than 26%. They reported that for $Ni_{(111)}$–Fe alloys containing more than 39% iron, adsorption of CO initially occurred via a dissociative mechanism and then subsequently molecular adsorption became the dominant

TABLE 5

The Influence of Reaction Temperature on the N_2 BET Surface Area of Carbon Filaments Grown on Selected Fe–Ni Catalysts during Interaction with CO/H_2 (4 : 1)

Temperature (°C)	Fe : Ni (6 : 4) surface area (m^2/g)	Fe : Ni (4 : 6) surface area (m^2/g)
500	194.3	180.0
575	—	93.4
600	94.7	109.9
650	77.2	82.8
700	—	41.4
750	31.9	—

form. In contrast, when the iron content in the alloy was below 26% molecular adsorption of CO was the exclusive mode. These observations were rationalized according to the notion that a cluster of iron atoms was required in order to dissociate the CO molecule and that such an event could not take place over a single iron atom. This argument lead to the postulate that in Fe–Ni alloys containing low concentrations of iron such atoms are randomly dispersed over the surface, and as a consequence, dissociation of CO is not a facile process.

In a number of studies the properties of Fe–Ni alloys have been correlated to the electronic structure of the valence band (39–42). Lawniczak-Jablonska and Auleytner (39, 40) found that changes in both the magnetic moment and the electronic specific heat were directly related to the electronic structure of the various alloys. One very interesting feature of these investigations was that the Fe–Ni (25 : 75) alloy exhibited unusual properties due to the formation of an intermetallic, Ni_3Fe. The formation of this compound gives rise to ordering, which results in significant changes in the electronic structure of the alloy. Investigations carried out by Chourasia and Chopra (41) on this particular Fe–Ni alloy led to the claim that there was a charge transfer from the Fe to Ni in this system. Furthermore, soft X-ray studies indicated that the surface composition of the alloy was enriched with Fe when compared to that of the bulk. Even though the present studies were carried out under somewhat different conditions to those highlighted above, it is conceivable that the presence of an electronic interaction exists between the two metals during the decomposition of CO.

Influence of hydrogen on carbon deposition. The decomposition of CO over the Fe–Ni powders in the absence of hydrogen at 600°C was found to be an extremely slow process. While there were no detectable gas phase products, the weight of the catalyst powder doubled after 3.5 h on stream due to the accumulation of solid carbon. Hydrogen has been reported to initiate the decomposition of carbon containing gases over selected transition metals and to have a distinct effect on the structural characteristics of the carbon filaments produced on the catalyst powder (4, 6, 13). It is evident from Fig. 2 that the introduction of as little as 20% hydrogen into the feed results in a significant increase in the amount of carbon deposited on the Fe–Ni powders, this behavior being particularly pronounced for catalysts containing more than 25% iron. The exact amount of hydrogen required to bring about this enhancement in catalytic activity is highly dependent upon the bimetallic composition as seen in Fig. 2.

The initial increase in carbon production is due to the CO hydrogenation reaction, with water being produced as a by-product and this feature, which has been reported previously has been attributed to various factors. Walker and co-workers (43) investigated the formation of filamentous carbon from the iron/CO system and suggested that the presence of a critical amount of hydrogen was necessary to decompose inactive iron carbides into the catalytically active metallic form. Other explanations for this phenomenon have centered around the ability of hydrogen either to maintain a reasonably clean metal surface by gasification residual carbon species (44) or to mutually enhance the adsorption of CO at the exposed metal faces (8).

While the arguments presented above may have validity with regard to the iron catalyzed decomposition of CO/H_2 mixtures, they may not all be applicable to the interaction Fe–Ni powders with the same reactant. Indeed, Mössbauer studies by Raupp and Delgass (45) on Fe–Ni catalysts reacted in CO/H_2 environments showed no evidence for carbide formation. Therefore the rationale that hydrogen was responsible for the conversion of carbide to metal is not germane to the bimetallic system. The current results show that as the concentration of hydrogen in the feed is increased so the CO hydrogenation reaction becomes more prominent, as evidenced from the progressive increase in the yield of water. In addition, hydrogen plays a diverse role in the production of solid carbon; at low levels it exerts a promotional effect on the formation of this product and at concentrations above 30% of the feed it acts as an inhibitor for carbon deposition. This factor along with the concomitant increase in the yield of methane at these higher hydrogen concentrations would suggest that an appreciable amount of the solid carbon produced under these conditions is simultaneously hydrogasified to methane.

Catalyst deactivation phenomenon. There appears to be an upper temperature limit for the production of carbon filaments in reasonable quantities from the Fe–Ni catalyzed decomposition of CO/H_2, which is dependent to a large degree on the composition of the bimetallic, as shown in Figs. 4 and 5. Nickel-rich powders tend to produce the maximum amount of solid carbon at a somewhat lower temperature than those in which iron is the major component. In all cases when the temperature is raised above this optimum level the bimetallic powders exhibit a sharp decline in catalytic activity. On subsequent lowering of the temperature to a previously active regime, restoration of the catalytic activity to the original value is observed. It is evident therefore, that the deactivation of these bimetallic systems cannot be attributed to the formation of a carbonaceous overlayer since the catalyst could not regain its activity simply by decreasing the temperature since the active sites would still be blocked.

A more plausible explanation may lie in the argument that at higher temperatures (725°C) some form of segregation might be induced where the surface tends to become enriched in nickel, a condition that does not favor the dissociative chemisorption of CO, as was shown in Fig. 1 and from previous studies (13, 47). Moreover, even when conditions are achieved that favor carbon deposition on nickel, the reactions leading to this step only occur on particular crystallite faces (48–50). Wandelt and Ertl (51) used soft X-ray appearance potential spectroscopy to study the behavior of a series of iron–nickel alloys. They reported that following heating of the alloys there was a significant increase in the appearance potential of the nickel whereas the values for iron remained practically unaffected. These data were interpreted in terms of a model where the surfaces of the alloy were enriched in nickel. The same conclusion was reached from theoretical calculations performed by Chelikowsky (52), which predict that nickel will preferentially segregate of the surface of an iron–nickel alloy in a reducing environment. A further factor that could have an impact on this proposed segregation effect is the tendency for iron-rich Fe–Ni particles to wet and spread along graphite edges when heated in the presence of hydrogen (35). This behavior highlights the potential for the formation of a strong interaction between certain bimetallic compositions and the graphite platelets constituting the filament structure produced at the carbon depositing faces of the catalyst particle. Under these circumstances it is not unreasonable to predict that any excess nickel atoms will tend to accumulate at the exposed faces of the catalyst particles.

Upon lowering of the temperature the strength of the interfacial reaction between the two components will decreased and the bimetallic particles recovered their initial surface composition, thereby allowing for the re-establishment of conditions that favor growth of carbon filaments. Indeed, as the reaction temperature was gradually decreased, it was seen that the activity of the catalyst recovered in step-wise fashion suggesting that the iron was slowly migrating to the surface. We intend to investigate the origin of this reversible deactivation step in more detail using *in situ* electron diffraction techniques to probe the pattern of behavior exhibited by particles derived from various Fe–Ni mixtures on single crystal graphite when heated in CO and CO/H_2 environments.

Kim and co-workers (12) studied carbon filament formation from the Cu–Ni catalyzed decomposition of an ethylene–hydrogen reactant mixture and reported the existence a similar deactivation phenomenon to that found in the present work. These authors concluded that there was an upper temperature limit of approximately 725°C for filament growth from this system. Above this temperature, the catalyst activity was very low and this behavior was attributed to the preferentially segregation of copper to the particle surface. As in the present case, when the reaction temperature was subsequently decreased, the activity of the catalyst was regained. Clearly, the presence of this type of reversible deactivation effect play an important role in a large number of reactions where bimetallics are used as the catalytic entities.

CO chemisorption studies on iron–nickel powders. The results of the chemisorption of CO onto the surfaces of Fe–Ni alloys performed in this investigation are very similar to those found by Vreeberg and co-workers (8, 9). From the numerous studies of CO interactions with surfaces of pure iron and nickel it was found that the gaseous molecules would only adsorb dissociatively on an iron cluster and not on single iron particles (9, 25, 46). In the case of nickel, CO dissociation is very sensitive to both the temperature and crystallographic orientation of the metal. It was demonstrated that a $Ni_{(100)}$ surface will dissociate carbon monoxide only at temperatures greater than 150°C, whereas a $Ni_{(111)}$ surface will only perform this step when it contains some defects.

It is reasonable to assume that there were very few or no iron clusters present in the reduced Fe–Ni (2 : 8) sample at any temperature since in this case CO dissociation was not observed and consequently one may conclude that the iron is very well dispersed throughout the nickel. For a catalyst with a slightly higher iron content, Fe–Ni (3 : 7), again no CO dissociation could be observed under these conditions at ambient temperature in agreement with the studies of Vreeberg and co-workers (8, 9). At 200°C, CO dissociation took place initially on the surface before adsorption became molecular in nature. This change in CO adsorption characteristics could account for the very differnt decomposition behavior observed on bimetallic powders where the nickel content was >75%. In such systems the CO will only exhibit molecular adsorption on the catalyst surface, and therefore, the decomposition of the reactant and formation of filamentous carbon will be very slow. On the other hand, with iron-rich bimetallic powders the dissociatively adsorbed CO will readily undergo decomposition and formation of filamentous carbon will be a facile process.

Structural characteristics of the solid carbon products. Carbon filaments grown during the decomposition of CO/H_2 mixtures over a pure iron catalyst have a uniform structure where the layers of graphitic carbon are stacked on top of each other in a similar manner to “a deck of cards,” Figs. 7a, b. The addition of nickel to iron induces major modifications in the structural characteristics of carbonaceous deposit. As the nickel content of the catalyst powder is increased, the degree of crystalline perfection of the filaments, as determined by temperature programmed oxidation and high resolution transmission electron microscopy, decreases perceptibly. The graphitic nature of the carbon filaments is dictated to a large degree by the wetting properties that exist between the metal and deposit. The formation of carbon filaments with a high degree of crystalline perfection has been shown to be due to the existence of a strong interaction between the two components (12). This condition is achieved under circumstances where the interstitial spacing in the metal faces matches the interatomic distance of the carbon–carbon bond of graphite. In this regard the orientation of the catalyst particle at the metal/carbon interface becomes a key factor in the control of the crystallinity of the deposited structure (53).

Studies performed by controlled atmosphere electron microscopy demonstrated that while Fe–Ni particles containing equal amounts of both metals exhibited a tendency to form a strong interaction with graphite when reacted in hydrogen, nickel-rich particles did not show the same behavior (35). These observations are consistent with present findings from temperature programmed oxidation studies that indicate a decrease in the graphitic nature of the carbon filaments that are generated from bimetallic powders where nickel is the major component. It is possible that the addition of large amounts of nickel to the iron catalyst may lead to a reconstruction of the carbon precipitating faces of the particle, from one, where the atomic arrangement of metal atoms is in register with the carbon atoms in graphite, to another, where these conditions are not so well matched. As the nickel content in the bimetallic increases these faces will predominate and the filamentous structures will become progressively more disordered.

The carbon filaments produced from a given bimetallic catalyst were found to become more graphitic in nature as the hydrogen content of the reactant gas was increased, Fig. 14. It is possible that the presence of excess hydrogen in the feed could induce the reconstruction of the bimetallic particles to generate faces where precipitation of carbon in the form of graphite was favored. Transmission electron microscopy examinations of catalyst particles associated with the filamentous structures showed that they tended to become more highly faceted as the hydrogen content in the reactant was increased. A further contributing factor is that hydrogen is known to enhance the wetting properties of Fe–Ni particles on a carbonaceous substrate, thereby inducing the formation of a strong interaction between the two components (35).

Examination of the structure of the deposit formed at reaction temperatures in excess of 600°C revealed the presence of a graphitic shell-like constituent that appeared to encapsulate some of the Fe–Ni particles. The existence of this type of material was first reported by Audier and coworkers (36–38) from studies of the decomposition of a CO/H_2 mixture over an Fe–Ni (1 : 3) catalyst at temperatures above 550°C. They attributed the formation of these graphite shells to a change in the fragmentation mechanism of the starting catalyst powder and it was significant that with a Fe–Ni (4 : 6) catalyst temperatures in excess of 650°C were required in order to produce this type of deposit. In more recent years other workers have reported the existence of similar growth structures from the interaction of CO with supported nickel and cobalt particles at 600°C (54) and from the decomposition of ethane over Fe–Ni alloy particles at 865°C (55). While the presence of sulfur species in the gaseous reactant appeared to enhance the formation of this type of deposit no clear understanding of the mechanistic features surrounding the growth process has emerged.

CONCLUSIONS

We have found that the composition of Fe–Ni catalysts can have a dramatic effect on the activity for the decomposition of CO/H_2 mixtures at 600°C The addition of an extra 5% nickel to a Fe–Ni (30 : 70) catalyst resulted in a decrease in the conversion of CO from 44.5 to 6.5% and a corresponding drop in the amount of solid carbon from 21 to 3%. The ratio of the two components in the catalyst also has a major influence on both the structure and crystalline perfection of the carbon filaments produced during the reaction. Temperature-programmed oxidation studies of carbon filaments grown from various Fe–Ni bimetallic particles shows that as the nickel content of the catalyst is increased there is a concomitant decrease in the resistance to oxidation of the solid carbon, indicating that the material tends to become more amorphous in nature. These features are rationalized according to the notion that the addition of nickel to iron results in a reconstruction of the particle surfaces that leads to a diminution in the likelihood of iron atoms being nearest neighbors and the generation of atomic arrangements at carbon precipitating faces that do not favor the formation of graphite platelets in the deposited filamentous structures.

A reversible deactivation process was shown to exist for all these Fe–Ni catalysts. At high temperatures, 725°C, the bimetallics were unable to dissociate CO and therefore carbon filament growth ceased. It was postulated that under these circumstances the faces at which gas phase decomposition reactions took place were enriched in nickel and as a consequence, dissociative chemisorption of CO, a key step in the eventual formation of filamentous carbon did not occur. Upon lowering the temperature to a previously active regime, the original composition of the active surfaces are reestablished and conditions reached that once again allow for the growth of carbon filaments.

ACKNOWLEDGMENT

Financial support for this work was provided by the U.S. Department of Energy, Basic Energy Sciences, Grant DE-FG02-93ER14358.

REFERENCES

1. Bertolacini, R. J., and Pellet, R. J., "Catalyst Deactivation" (B. Delmon and G. E. Froment, Eds.), p. 73, Elsevier, Amsterdam, 1980.
2. Figoli, N. S., Beltramini, J. N., Querini, C. A., and Parera, J. M., *Appl. Catal.* **15**, 41 (1985).
3. Rodriguez, N. M., *J. Mater. Res.* **8**, 3233 (1993).
4. Sacco, A., Jr., "Carbon Fibres Filaments and Composites" (J. L. Figueiredo, *et al.*, Eds), p. 459, Kluwer Academic, Amsterdam, 1990.
5. Bartholomew, C. H., *Catal. Rev. Sci. Eng.* **16**, 155 (1977).
6. De Bokx, P. K., Kock, A. J. H. M., Boellaard, E., Klop, W., and Geus, J. W., *J. Catal.* **96**, 454 (1985).

7. Kock, A. J. H. M., De Bokx, P. K., Boellaard, E., Klop, W., and Geus, J. W., *J. Catal.* **96**, 468 (1985).
8. Boellaard, E., De Bokx, P. K., Kock, A. J. H. M., and Geus, J. W., *J. Catal.* **96**, 481 (1985).
9. Vreeburg, R. J., van de Loosdrecht, J., Gijzeman, O. L. J., and Geus, J. W., *Catal. Today* **10**, 329 (1991).
10. Boellaard, E., Vreeburg, R. J., Gijzeman, O. L. J., and Geus, J. W., *J. Mol. Catal.* **92**, 299 (1994).
11. Kim, M. S., Rodriguez, N. M., and Baker, R. T. K., *J. Catal.* **131**, 60 (1990).
12. Kim, M. S., Rodriguez, N. M., and Baker, R. T. K., *J. Catal.* **134**, 253 (1992).
13. Rodriguez, N. M., Kim, M. S., and Baker, R. T. K., *J. Catal.* **144**, 93 (1993).
14. Rodriguez, N. M., Chambers, A., and Baker, R. T. K., *Langmuir* **11**, 3862 (1995).
15. Bianchini, E. C., and Lund, C. R. F., *J. Catal.* **117**, 455 (1989).
16. Walker, P. L., Jr., Rakszawski, J. F., and Imperial, G. R., *J. Phys. Chem.* **63**, 133 (1959).
17. Davis, W. R., and Rigby, G. R., *Trans. Brit. Ceram. Soc.* **53**, 511 (1954).
18. Baker, R. T. K., Harris, P. S., Thomas, R. B., and Waite, R. J., *J. Catal.* **30**, 86 (1973).
19. Turkdogan, E. T., and Vinters, J. V., *Met. Trans.* **5**, 11 (1974).
20. Stewart, I., Tricker, M. J., and Cairns, J. A., *J. Catal.* **94**, 360 (1985).
21. Pijolat, M., Perrichon, V., and Bussière, P., *J. Catal.* **107**, 82 (1987).
22. Dry, M. E., Shingles, T., Boshoft, L. T., and Botha, C. S. van H., *J. Catal.* **17**, 347 (1970).
23. Karcher, W., and Glaude, P., *Carbon* **9**, 617 (1971).
24. Trimm, D. L., *Catal. Rev. Sci. Eng.* **16**, 155 (1977).
25. Zdonik, S. B., Green, G. J., and Hallee, L. P., "Manufacturing Ethylene," Petroleum Publ. Co., Tulsa, OK, 1970.
26. Gijzemann, O. L. J., Vink, T. J., van Pruissen, O. P., and Geus, J. W., *J. Vac. Sci. Technol.* **5**, 718 (1987).
27. Vink, T. J., van Zandvoort, M. M. J., Gijzemann, O. L. J., and Geus, J. W., *Appl. Surf. Sci.* **18**, 255 (1984).
28. Gijzemann, O. L. J., van Zandvoort, M. M. J., and Labohm, F., *J. Chem. Soc. Faraday Trans. II* **80**, 771 (1984).
29. Yates J. T., Jr., Goodman, D. W., and Madey, T. E., "Proc. 7th Intern. Congr. and 3rd Intern. Conf. on Solid Surfaces, 1977," p. 1133.
30. Vorburger, T. V., Sandstrom, D. R., and Waclawski, B. J., *Surf. Sci.* **60**, 211 (1976).
31. Froitzheim, H., Ibach, H., and Lehwalw, S., *Surf. Sci.* **63**, 56 (1977).
32. Textor, M., Gay, I. D., and Mason, R., *Proc. Roy. Soc. A* **356**, 37 (1977).
33. Goodman, D. W., Madey, T. E., and Yates J. T., Jr., *J. Catal.* **50**, 279 (1977).
34. Best, R. J., and Russell, W. W., *J. Am. Chem. Soc.* **76**, 838 (1954).
35. Baker, R. T. K., Chludzinski, J. J., and Sherwood, R. D., *Carbon* **23**, 245 (1985).
36. Audier, M., Guinot, J., Coulon, M., and Bonnetain, L., *Carbon* **19**, 99 (1981).
37. Audier, M., and Coulon, M., *Carbon* **23**, 317 (1985).
38. Audier, M., Oberlin, A., Oberlin, M., Coulon, M., and Bonnetain, L., *Carbon* **19**, 217 (1981).
39. Lawniczak-Jablonska, K., and Auleytner, J., *J. Phys. F: Met. Phys.* **12**, 2523 (1982).
40. Lawniczak-Jablonska, K., and Auleytner, J., *J. Phys. F: Met. Phys.* **12**, 2729 (1982).
41. Chourasia, A. R., and Chopra, D. R., *Surf. Sci.* **206**, 484 (1988).
42. Calvayrac, Y., and Fayard, M., *Phys. Stat. Sol. (A)* **17**, 407 (1973).
43. Walker, P. L., Jr., Rakszawski, J. F., and Imperial, G. R., *J. Phys. Chem.* **63**, 140 (1959).
44. Nishiyama, Y., and Tamai, Y., *J. Catal.* **45**, 1 (1976).
45. Raupp, G. B., and Delgass, W. N., *J. Catal.* **58**, 348 (1979).
46. Vink, T. J., Gijzemann, O. L. J., and Geus, J. W., *Surf. Sci.* **150**, 14 (1985).
47. Sacco, A., Jr., Geurts, F. W. A. H., Jablonski, G. A., Lee, S., and Gateley, R. A., *J. Catal.* **119**, 322 (1989).
48. Leidheiser, H., Jr., and Gwathmey, A. T., *J. Amer. Chem. Soc.* **70**, 1206 (1948).
49. Kehrer, V. J., and Leidheiser, H., Jr., *J. Phys. Chem.* **58**, 550 (1954).
50. Renshaw, G. D., Roscoe, C., and Walker, P. L., Jr., *J. Catal.* **22**, 394 (1971).
51. Wandelt, K., and Ertl, G., *J. Phys. F. Metal Phys.* **6**, 1607 (1976).
52. Chelikowsky, J. R., *Surf. Sci.* **139**, 1197 (1984).
53. Yang, R. T., and Chen, J. P., *J. Catal.* **115**, 52 (1989).
54. Nolan, P. E., Lynch, D. C., and Cutler, A. H., *Carbon* **32**, 477 (1994).
55. Rodriguez, N. M., Kim, M. S., Fortin, F., Mochida, I., and Baker, R. T. K., *Appl. Catal.* **148**, 265 (1997).